A General Linear Least Squares SDOF Algorithm for Identifying Eigenvalues and Residues

J. H. Ginsberg, M. Allen, A. Ferri, and C. Moloney
The G. W. Woodruff School of Mechanical Engineering
Georgia Institute of Technology Atlanta, GA 30332-0405

October 2, 2002

Abstract

Large damping levels, low signal to noise ratio, and low frequency resolution can cause difficulties for current SDOF SISO algorithms that identify natural frequency, modal damping ratio, and the residue associated with each eigenvalue. This paper offers an alternative technique that through a change of variables leads to a set of linear equations for the complex eigenvalue and residue. The approach resembles the least-squares procedure described by Phillips and Allemang [Proc. 14th International Modal Analysis Conference, 1996], but it avoids the approximation that the complex conjugate residue is unimportant. For noise-free data, the procedure yields the exact parameters from FRF values at any two frequencies. Noisy data is readily addressed by implementing linear least-squares. The paper uses synthetic FRF data contaminated by 20% white-noise to assess the performance via Monte Carlo simulation. Mean values and standard deviations of the eigenvalue and residue are computed for several sampling rates. An effective criterion for selecting data points to be between the quarter-power points of a resonance peak is demonstrated to be a good criterion in each case.

NOMENCLATURE

$G_{jP}(\omega)$	Displacement transfer function
A	Modal residue
λ	Modal eigenvalue
$A_r,\ A_i$	Real and imaginary parts of A
$\alpha,\ \beta$	Real and imaginary parts of λ
Ω	Undamped natural frequency
δ	Cutoff factor for data points, see eq. (18)
N	Number of data points for least squares fit
$E[\,]$	Mean value of a quantity
$\sigma[\,]$	Standard deviation of a quantity
ω	Drive frequency
$\Delta\omega$	Frequency sampling interval

1 INTRODUCTION

Algorithms for experimental modal analysis are categorized as to whether they are SDOF (single-degree-of-fredom) or MDOF (multi-degree-of-fredom) , which refers to whether identification of the modal properties allows for the contribution to the data being processed of several modes. For some systems, especially those that are very lightly damped, SDOF techniques often suffice, especially if one restricts their attention to the lower frequency modes. SDOF techniques also can be used to estimate modal properties as a check for an MDOF identification. Another use for SDOF identification is as a component of an MDOF algorithm. Such is the case for the iterative AMI (Algorithm of Mode Isolation) procedure, which synthesizes the modal picture as sequence of SDOF steps.

There are a multitude of SDOF algorithms; Ewins [1] and Maia *et al* [2] provide extensive surveys, and Allemang [3] gives a concise review of the more common ones. All techniques are inherently restricted to working with frequency domain data. They also are inherently approximate, because they ignore the presence of other modes. However, they contain other approximations, depending on the characteristics of the complex frequency response (FRF) on which they are based. For example, one can identify the natural frequency as the frequency at which the FRF has its maximum magnitude, the frequency at which the real part of the FRF is zero, the frequency at which points on a Nyquist plot of the FRF have their maximum spacing, or the frequency at which the distance from a point on a Nyquist plot to the midpoint between the high and low frequency limits is a maximum .

Even if one considers analytical data uncontaminated by noise, results obtained by different SDOF techniques will not be the same. A primary reason for discrepancies is the usage of different models. The earlier formulations, such

as Peak Amplitude, Maximum Quadrature, and Maximum Frequency Spacing, were founded on a real modal analysis incorporating modal damping. Later developments were founded on complex modal analysis, which is exact for arbitrary viscous damping. Furthermore, some MDOF versions using either type of modal description are adapted to work with structural damping. An additional cause for discrepancy, although one that is readily rectified, is semantic in nature, stemming from the fact that the meaning of natural frequency is unambiguous only for proportionally damped systems. The fineness of the frequency increment also affects the result obtained by some techniques. For example, in the Maximum Frequency Spacing method the frequency increment determines precision to which the maximum spacing between adjacent points may be resolved. The difference between modal parameter estimates obtained from the various techniques are generally insignificant for low-noise data obtained from lightly damped systems. However, some of the available SDOF techniques are more robust than others, that is, they tend to behave better when applied to FRF data that has significant levels of noise.

This paper offers an alternative technique that through a change of variables leads to a set of linear equations for the complex eigenvalue and complex residue. The approach resembles the linear least-squares procedure described by Phillips and Allemang [3], but it avoids the approximation that the complex conjugate residue is unimportant. From a philosophical perspective, the SDOF algorithm outlined in the following is akin Dobson's extension of the inverse method [5], in that both yield exact results if the FRF data is noise-free and other modes actually are not present. The present approach is founded on the analytical representation of a single complex mode and its conjugate to the FRF of a system with arbitrary viscous damping, while Dobson's method is exact for the case of structural damping. Unlike Dobson's method, only two FRF values are required to obtain exact values of the complex eigenvalue and residue factor in the ideal noise-free case, with results derived by solving two pairs of simultaneous algebraic equations. Dobson's method accounts for the presence of a residual term associated with other modes, but does so by considering the term to be constant over the frequency interval being processed. Such an approximation is likely to be acceptable only if the natural frequencies are well separated, so it is not believed that the omission of such a term from the present formulation is significant. Extension of the method to noisy data is achieved by implementing a linear least squares procedure using FRF values in the frequency range where the FRF exhibits a maximum. After the method is described, consideration is given to the selection of frequency increment and interval for the FRF data in a noisy environment. Because the algorithm in the noise-free case is exact for arbitrary levels of damping, provided that the mode is underdamped, a heavy-damping case is included for the sake of completeness. The data for the present study is computed analytically, to which is added white noise scaled as a fraction of the peak FRF magnitude. The effectiveness of the procedure for measured data obtained from a square plate is the subject of a companion paper [6].

2 ANALYTICAL DEVELOPMENT

The starting point for the derivation is the contribution of a single underdamped complex mode and its conjugate to the FRF of generalized coordinate q_j resulting from unit harmonic excitation of generalized coordinate P,

$$G_{jP}(\omega) = \frac{A}{i\omega - \lambda} + \frac{A^*}{i\omega - \lambda} \tag{1}$$

The eigenvalue λ and residue A are decomposed into their real and imaginary parts, such that

$$A = A_r + iA_i, \quad \lambda = -\alpha + i\beta \tag{2}$$

With this, the FRF becomes

$$G_{jP}(\omega) = 2\frac{(i\omega + \alpha)A_r - \beta A_i}{\alpha^2 + \beta^2 - \omega^2 + 2i\alpha\omega} \tag{3}$$

The next step is to introduce a change of variables,

$$u = \alpha^2 + \beta^2 \tag{4}$$

Clearing the denominator in eq. (3) and breaking the result into real and imaginary parts then leads to

$$(G(\omega))\left(u - \omega^2\right) - 2\omega\alpha\,\mathrm{Im}(G(\omega)) = 2(\alpha A_r - \beta A_i) \tag{5}$$

$$\mathrm{Im}(G(\omega))\left(u - \omega^2\right) + 2\omega\alpha\,\mathrm{Re}(G(\omega)) = 2\omega A_r \tag{6}$$

If this pair of real equations are evaluated at two arbitrary frequencies, the result is four simultaneous equations for u, α, A_r, and A_i.

Solution of eqs. (5) and (6) is expedited by the fact that both equations are linear in u and α, and the second is also linear in A_r. Let ω_1 and ω_2 denote two arbitrary frequencies, and let $G_k \equiv G(\omega_k)$. Evaluation of eq. (6) at both frequencies gives

$$[X]\left\{\begin{array}{c} u \\ \alpha \end{array}\right\} = A_r \left\{\begin{array}{c} 2\omega_1 \\ 2\omega_2 \end{array}\right\} + \left\{\begin{array}{c} \omega_1^2\,\mathrm{Im}(G_1) \\ \omega_2^2\,\mathrm{Im}(G_2) \end{array}\right\} \tag{7}$$

where

$$[X] = \left[\begin{array}{cc} \mathrm{Im}(G_1) & 2\omega_1\,\mathrm{Re}(G_1) \\ \mathrm{Im}(G_2) & 2\omega_2\,\mathrm{Re}(G_2) \end{array}\right] \tag{8}$$

Similarly, eq. (5) evaluated at both frequencies yields

$$[Y]\left\{\begin{array}{c} u \\ \alpha \end{array}\right\} = 2\left(\alpha A_r - \beta A_i\right)\left\{\begin{array}{c} 1 \\ 1 \end{array}\right\} + \left\{\begin{array}{c} \omega_1^2 \operatorname{Re}(G_1) \\ \omega_2^2 \operatorname{Re}(G_2) \end{array}\right\} \tag{9}$$

where

$$[Y] = \left[\begin{array}{cc} \operatorname{Re}(G_1) & -2\omega_1 \operatorname{Im}(G_1) \\ \operatorname{Re}(G_2) & -2\omega_2 \operatorname{Im}(G_2) \end{array}\right] \tag{10}$$

Elimination of u and α between eqs. (7) and (9) leads to a pair of linear equations for $\alpha A_r - \beta A_i$ and A_r. Back-substitution of these values into either of the aforementioned equations yields u and α, which then may be used to extract A_i from the computed value of $\alpha A_r - \beta A_i$. After both parts of the eigenvalue have been computed, the corresponding undamped modal natural frequency Ω and modal damping ratio ζ can be obtained from

$$\lambda = -\zeta\Omega + \left(1-\zeta^2\right)^{1/2} i \implies \Omega = u^{1/2}, \quad \zeta = \frac{\alpha}{u^{1/2}} \tag{11}$$

The procedure outlined thus far is suitable only if the FRF is noise-free. Extension of the technique to a linear least squares procedure capable of handling noisy data is straightforward. The first step is to extend the definitions of the matrices to include values obtained at a number of frequencies. For brevity, define

$$\begin{aligned}
[X] &= \left[\begin{array}{cc} \operatorname{Im}(G_1) & 2\omega_1 \operatorname{Re}(G_1) \\ \operatorname{Im}(G_2) & 2\omega_2 \operatorname{Re}(G_2) \\ \vdots & \vdots \end{array}\right] \\
[Y] &= \left[\begin{array}{cc} \operatorname{Re}(G_1) & -2\omega_1 \operatorname{Im}(G_1) \\ \operatorname{Re}(G_2) & -2\omega_2 \operatorname{Im}(G_2) \\ \vdots & \vdots \end{array}\right] \\
\{\omega\} &= \left\{\begin{array}{c} \omega_1 \\ \omega_2 \\ \vdots \end{array}\right\} \\
\left\{\omega^2 \operatorname{Re}(G)\right\} &= \left\{\begin{array}{c} \omega_1^2 \operatorname{Re}(G_1) \\ \omega_2^2 \operatorname{Re}(G_2) \\ \vdots \end{array}\right\} \\
\left\{\omega^2 \operatorname{Im}(G)\right\} &= \left\{\begin{array}{c} \omega_1^2 \operatorname{Im}(G_1) \\ \omega_2^2 \operatorname{Im}(G_2) \\ \vdots \end{array}\right\}
\end{aligned} \tag{12}$$

where the number of rows for each quantity is the number of data points N used for the identification.

The extended version of eq. (7) is considered to be an over-determined set of linear equations for u and α. Requiring that they be satisfied in a linear least squares sense leads to

$$\left\{\begin{array}{c} u \\ \alpha \end{array}\right\} = \left[\hat{X}\right]^{-1} [X]^{\mathrm{T}} \left\{2\{\omega\} A_r + \left\{\omega^2 \operatorname{Im}(G)\right\}\right\} \tag{13}$$

When this expression is substituted into the extended version of eq. (5), the result is

$$\begin{aligned}
&2[Y]\left[\hat{X}\right]^{-1}[X]^{\mathrm{T}}\{\omega\} A_r \\
&\quad + [Y]\left[\hat{X}\right]^{-1}[X]^{\mathrm{T}}\left\{\omega^2 \operatorname{Im}(G)\right\} \\
&\quad = \left\{\omega^2 \operatorname{Re}(G)\right\} + 2\left(\alpha A_r - \beta A_i\right)\{1\}
\end{aligned} \tag{14}$$

The preceding expression represents an overdetermined set of linear equations for the two unknowns $2\left(\alpha A_r - \beta A_i\right)$ and A_r. To solve them in a least squares sense, define

$$[Z] = \left[\begin{array}{c|c} 2[Y]\left[\hat{X}\right]^{-1}[X]^{\mathrm{T}}\{\omega\} & -2\{1\} \end{array}\right] \tag{15}$$

which enables one to write

$$\begin{aligned}
\left\{\begin{array}{c} A_r \\ \alpha A_r - \beta A_i \end{array}\right\} = &\left[\hat{Z}\right]^{-1}\left[\hat{Z}\right]\left\{\left\{\omega^2 \operatorname{Re}(G)\right\}\right. \\
&\left. - [Y]\left[\hat{X}\right]^{-1}[X]^{\mathrm{T}}\left\{\omega^2 \operatorname{Im}(G)\right\}\right\}
\end{aligned} \tag{16}$$

Substitution of the value of A_r obtained from this relation into eq. (13) yields α and u, from which β may be obtained by returning to eq. (4). Finally, the value of A_i is found by substituting the other parameters into the value of $\alpha A_r - \beta A_i$ found from the preceding, while the modal natural frequency and damping ratio are obtained from eqs. (11).

3 EVALUATION

The procedure that follows will consider a specific complex mode and its complex conjugate. Because only one mode is to be considered the frequency scale and magnitude of the residue will not affect the quality of the identification, provided that the noise scales in the same way as the residue. Therefore the undamped natural frequency will be taken to be $\Omega = 1$. Several evaluations indicated that the phase angle of the residue also is unimportant, so the value $A = -2 + 2.3i$ was held constant. (A phase angle for the residue that is not close to either 0 or π is inconsistent with light damping. However, one of the issues to be considered is the quality of identification as ζ is increased to heavy damping. Also, identifying a highly complex value of A is no easier than identifying a value that is nearly real.) The FRF data set is obtained by evaluating the analytical $G(\omega)$ according to eq. (1). The values at each of a sequence of equispaced frequencies is contaminated by white-noise scaled by the maximum value of $G(\omega)$, specifically,

$$\begin{aligned}
G_{\text{noise}}(\omega_k) = \; &G(\omega_k) + \varepsilon \max\left(\left|G(\omega_k)\right|\right) \times \\
&\left[\operatorname{rnd}(-1,1) + i \operatorname{rnd}(-1,1)\right]
\end{aligned} \tag{17}$$

where rnd$(-1, 1)$ represents a random number uniformly distributed between -1 and 1, newly generated at each evaluation. Most computations will consider $\varepsilon = 0.2$, which corresponds to a minimum signal to noise ratio of 14 dB at the peak FRF.

Because the best signal to noise ratios are obtained in the range of the peak FRF, it is reasonable to focus on the FRF values in that region for the identification. There are a number of parameters affecting the quality of the identification. For a given value of ζ and ε, the frequency increment determines how well the peak FRF is resolved. Three cases will be considered: $\Delta\omega = 0.5\zeta\Omega$, which corresponds to a fine frequency sweep in which the sampling interval is 25% of the modal bandwidth, $\Delta\omega = \zeta\Omega$ which represents a reasonably good sampling of the peak FRF, and $\Delta\omega = 2\zeta\Omega$, where the sampling is barely adequate. Once the sampling interval is set, one needs to consider the number of points to use for the least squares evaluation. Here one encounters a trade-off. If many points are selected, there will be more opportunity to average out the effect of errors. However, increasing the number of points with the sampling interval held fixed introduces points that are increasingly far from the peak, and therefore have a lower signal to noise ratio. The evaluations presented here selected all points in a frequency band surrounding the peak FRF value. The lower and upper frequency limits were set as the minimum and maximum frequency, respectively, at which

$$|G_{\text{noise}}(\omega_k)| \geq \delta \max(|G_{\text{noise}}(\omega_k)|) \tag{18}$$

The evaluations used $\delta = 0.71$, 0.50, and 0.35, corresponding to amplitude limits that that are respectively -3 dB, -6 dB, and -9 dB relative to the peak. For each set of parameters, the linear least squares procedure was carried out as a Monte Carlo simulation using 30 different sets of random noise.

Figure 1 depicts a typical data set for used for one least squares evaluation. The second graph in this figure depicts the frequency bands associated with the three values of δ. The first set of evaluations considered three damping ratios representative of light damping, $\zeta = 0.005$, moderate damping, $\zeta = 0.03$, and heavy damping, $\zeta = 0.20$. The values of λ and A were identified for each randomized FRF, and the mean value, $E[\,]$, and standard deviation, $\sigma[\,]$ of both quantities was computed. Results for the light damping case are described in Tables 1 to 3, with the sequence corresponding to progressively decreasing values of $\Delta\omega$.

In the light damping case the best overall results, in terms of agreement of the average estimate for the eigenvalue and residue, as well as the size of the standard deviations,

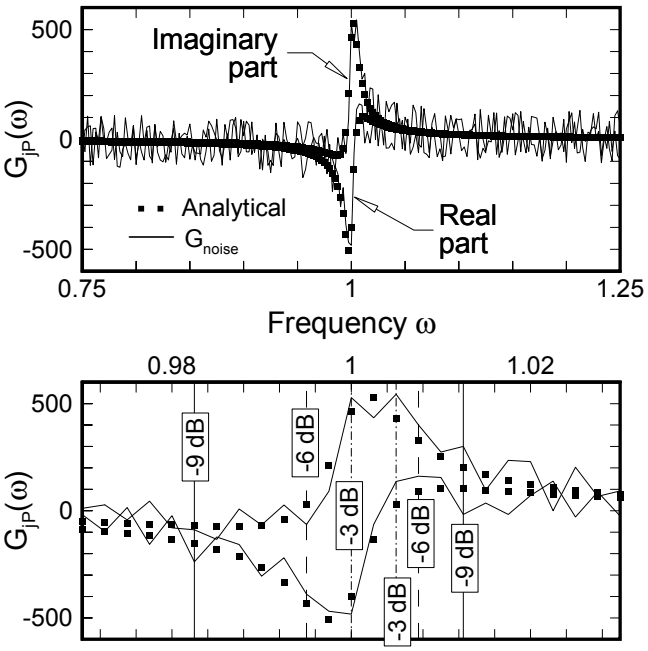

Figure 1: $G_{jP}(\omega)$ and $G_{\text{noise}}(\omega)$ when $\Omega = 1$, $\zeta = 0.005$, $A = -2 + 2.3i$, $\varepsilon = 0.20$, and $\Delta\omega = 0.5\zeta\Omega$.

are obtained by cutting off the data at -6 dB relative to the peak (Table 2). When the input data values are selected to fit this criterion, the smallest standard deviations of both parts of the eigenvalue and residue are obtained when the frequency increment is one quarter of the bandwidth. The corresponding errors in the mean values of the eigenvalue are 0.02% for the imaginary part ("damped natural frequency") and 5% for the real part (damping ratio), while the mean values of both parts of the residue are both less than 4% different from the respective true values.

In the moderate damping case the results obtained using

$\delta(dB)$	-3	-6	-9
N (average)	2.033	2.13	4.63
$E[\text{Re}(\lambda)]$	-0.00495	-0.00505	-0.00573
$E[\text{Im}(\lambda)]$	1.00036	0.99975	0.99958
$\sigma[\text{Re}(\lambda)]$	0.00136	0.00138	0.00216
$\sigma[\text{Im}(\lambda)]$	0.00142	0.00189	0.00455
$E[\text{Re}(A)]$	-1.90975	-2.19162	-2.26479
$E[\text{Im}(A)]$	2.38571	2.31945	2.74639
$\sigma[\text{Re}(A)]$	0.76261	1.03460	1.27882
$\sigma[\text{Im}(A)]$	0.80179	0.76523	0.96692

Table 1: Statistical results of the identification, l=-0.005+0.99999i, A=-2+2.3i, e=0.2, Dw=2zW.

$\delta(dB)$	-3	-6	-9
N (average)	2.40	4.20	7.83
$E[\mathrm{Re}(\lambda)]$	-0.00515	-0.00466	-0.00475
$E[\mathrm{Im}(\lambda)]$	0.99964	0.99972	1.00040
$\sigma[\mathrm{Re}(\lambda)]$	0.00103	0.00096	0.00104
$\sigma[\mathrm{Im}(\lambda)]$	0.00116	0.00106	0.00144
$E[\mathrm{Re}(A)]$	-2.2680	-2.0499	-1.9182
$E[\mathrm{Im}(A)]$	2.3756	2.3562	2.5315
$\sigma[\mathrm{Re}(A)]$	0.674	0.481	0.554
$\sigma[\mathrm{Im}(A)]$	0.537	0.436	0.430

Table 2: Statistical results of the identification, l=-0.005+0.99999i, A=-2+2.3i, e=0.2, Dw=zW.

$\delta(dB)$	-3	-6	-9
N (average)	3.83	7.87	16.57
$E[\mathrm{Re}(\lambda)]$	-0.00486	-0.00476	-0.00477
$E[\mathrm{Im}(\lambda)]$	0.99988	0.99983	0.99988
$\sigma[\mathrm{Re}(\lambda)]$	0.00110	0.00060	0.00069
$\sigma[\mathrm{Im}(\lambda)]$	0.00083	0.00090	0.00114
$E[\mathrm{Re}(A)]$	-2.1015	-2.06366	-2.06685
$E[\mathrm{Im}(A)]$	2.3090	2.3331	2.4249
$\sigma[\mathrm{Re}(A)]$	0.512	0.427	0.396
$\sigma[\mathrm{Im}(A)]$	0.490	0.323	0.303

Table 3: Statistical results of the identification, l=-0.005+0.99999i, A=-2+2.3i, e=0.2, Dw=0.5zW.

$\delta(dB)$	-3	-6	-9
N (average)	4.20	7.50	19.53
$E[\mathrm{Re}(\lambda)]$	-0.02864	-0.02953	-0.02971
$E[\mathrm{Im}(\lambda)]$	1.00023	1.00092	1.00139
$\sigma[\mathrm{Re}(\lambda)]$	0.00563	0.00458	0.00504
$\sigma[\mathrm{Im}(\lambda)]$	0.0052	0.0050	0.0122
$E[\mathrm{Re}(A)]$	-1.92261	-2.03182	-2.07687
$E[\mathrm{Im}(A)]$	2.38676	2.50286	2.46016
$\sigma[\mathrm{Re}(A)]$	0.400	0.376	0.443
$\sigma[\mathrm{Im}(A)]$	0.559	0.306	0.214

Table 4: Statistical results of the identification, l=-0.030+0.99955i, A=-2+2.3i, e=0.2, Dw=0.5zW.

$\delta(dB)$	-3	-6	-9
N (average)	3.73	9.47	16.43
$E[\mathrm{Re}(\lambda)]$	-0.19631	-0.20184	-0.18939
$E[\mathrm{Im}(\lambda)]$	0.99234	0.98657	0.97870
$\sigma[\mathrm{Re}(\lambda)]$	0.0440	0.0282	0.0290
$\sigma[\mathrm{Im}(\lambda)]$	0.0567	0.0418	0.0472
$E[\mathrm{Re}(A)]$	-1.91297	-1.96961	-2.06895
$E[\mathrm{Im}(A)]$	2.50656	2.51170	2.22505
$\sigma[\mathrm{Re}(A)]$	0.861	0.371	0.420
$\sigma[\mathrm{Im}(A)]$	0.687	0.402	0.397

Table 5: Statistical results of the identification, l=-0.2+0.97980i, A=-2+2.3i, e=0.2, Dw=0.5zW.

a -3dB cutoff and a frequency increment equal to the modal bandwidth appeared to be quite good. However, the cutoff criterion is such that only two data values near the peak FRF were used in the identification, which is the minimum possible. This would suggest that the good agreement is a matter of happenstance. Otherwise, the smallest standard deviations for the eigenvalues and residues were obtained once again when the cutoff is -6 dB and the frequency increment is one quarter the bandwidth. The results for this case are described in Table 4; the errors are 0.1% for $\mathrm{Im}(\lambda)$, 1.6% for $\mathrm{Re}(\lambda)$, and less than 9% for both parts of A. The situation for heavy damping is essentially the same, in that the lowest standard deviations are obtained with a cutoff of -6 dB and a frequency increment that is one quarter the bandwidth. The corresponding statistical results are described in Table 5. The errors are 0.7% for $\mathrm{Im}(\lambda)$, 0.9% for $\mathrm{Re}(\lambda)$, and less than 10% for both parts of A.

A trend identified from examination of the results for these three damping ratios is that for any frequency increment and cutoff, the best overall agreement is obtained for $\mathrm{Im}(\lambda)$ and the greatest disagreement is for A. In the best case the ratio of a standard deviation of either part of A to the mean value of A is essentially the noise parameter ε used to construct the FRF data, while the ratios of the standard deviations for both parts of λ with respect to their corresponding mean values is substantially less than ε. To demonstrate that these tendencies are typical, Table 6 displays the results obtained for moderate damping when the noise parameter is $\varepsilon = 0.05$ and the frequency increment is one quarter the bandwidth. With a -6 dB cutoff, the errors are 0.004% for $\mathrm{Im}(\lambda)$, 0.5% for $\mathrm{Re}(\lambda)$, and less than 1% for either part of A. The ratios of the standard deviations for the parts of λ to the mean values are much smaller than ε, while the standard deviation ratios for both parts of A are comparable to ε.

The last item for consideration is the effectiveness of the linear least squares scheme for structural damping. The standard form of a frequency response function for a system with structural damping is

$$G_{jp}(\omega) = \frac{U}{\Omega^2(1+i\gamma) - \omega^2} \tag{19}$$

where U is real, Ω is the undamped natural frequency, and γ is the loss factor. To identify the equivalent λ and A values, eq. (3) in the vicinity of $\omega^2 = \alpha^2 + \beta^2$, i.e. frequencies near the peak FRF, is matched to the

$\delta(dB)$	-3	-6	-9
N (average)	4.07	7.13	10.77
$E[\mathrm{Re}(\lambda)]$	-0.02971	-0.03014	-0.02995
$E[\mathrm{Im}(\lambda)]$	0.99950	0.99951	0.99970
$\sigma[\mathrm{Re}(\lambda)]$	0.00147	0.00103	0.00098
$\sigma[\mathrm{Im}(\lambda)]$	0.00126	0.00095	0.00105
$E[\mathrm{Re}(A)]$	-1.98355	-2.00757	-1.99708
$E[\mathrm{Im}(A)]$	2.28189	2.32264	2.31821
$\sigma[\mathrm{Re}(A)]$	0.125	0.094	0.069
$\sigma[\mathrm{Im}(A)]$	0.110	0.089	0.063

Table 6: Statistical results of the identification, l=-0.030+0.99955i, A=-2+2.3i, e=0.2, Dw=0.5zW.

$\delta(dB)$	-3	-6	-9
N (average)	2.00000	2.13333	4.16667
$E[\mathrm{Re}(\lambda)]$	-0.05220	-0.04892	-0.05468
$E[\mathrm{Im}(\lambda)]$	0.99800	0.99784	1.00162
$\sigma[\mathrm{Re}(\lambda)]$	0.01939	0.01717	0.01850
$\sigma[\mathrm{Im}(\lambda)]$	0.01593	0.01565	0.03027
$E[\mathrm{Re}(A)]$	0.02003	0.03952	-0.11475
$E[\mathrm{Im}(A)]$	-1.01319	-1.04851	-1.19037
$\sigma[\mathrm{Re}(A)]$	0.268	0.314	0.434
$\sigma[\mathrm{Im}(A)]$	0.349	0.302	0.235

Table 7: Statistical results of the identification, structural damping, g=0.10, U=1,l=-0.050+0.99875i, A=-1.00125i, e=0.2, Dw=2zW.

preceding. The two match to first order if

$$\begin{aligned} \left(\alpha^2+\beta^2\right)^{1/2} &= \Omega, \quad \alpha = \frac{1}{2}\gamma\Omega \\ A_r &= 0, \quad -\frac{\beta A_i}{\alpha} = \frac{U}{\gamma\Omega} \end{aligned} \tag{20}$$

which leads to

$$\begin{aligned} \lambda &= -\tfrac{1}{2}\gamma\Omega + \left(1-\tfrac{1}{4}\gamma^2\right)^{1/2}\Omega i \\ A &= -\frac{U}{\left(1-\frac{1}{4}\gamma^2\right)^{1/2}\Omega} i \end{aligned} \tag{21}$$

Each entry in Tables 7-9 describes the results of thirty runs with $\varepsilon = 0.2$ for various $\Delta\omega$ and δ corresponding to $\Omega = U = 1$, and $\gamma = 0.1$. The statistical trends are consistent with those in the previous cases. Once again, the best results are obtained with a frequency increment equal to half the modal bandwidth, with the data cutoff set at -6 dB. In that case the mean eigenvalue shows a smaller discrepancy relative to the true value than does the residue, with errors of 0.1% for $\mathrm{Im}(\lambda)$, 1 % for $\mathrm{Re}(\lambda)$, and 4% for both parts of A relative to the average value of $|A|$. Also, for any sampling scheme the ratio of the standard deviation to the corresponding mean value is smaller for $\mathrm{Im}(\lambda)$ than it is for $\mathrm{Re}(\lambda)$, and both are smaller than the ratios for A. As was found for the previous cases, the coarsest sampling (frequency increment equal to the bandwidth) leads to a ratio of the standard deviation of either part of A to the corresponding mean value that is approximately 2ε, but those values now drop well below ε for the finest sampling and optimal data cutoff.

$\delta(dB)$	-3	-6	-9
N (average)	2.47	3.97	9.43
$E[\mathrm{Re}(\lambda)]$	-0.04912	-0.05237	-0.04675
$E[\mathrm{Im}(\lambda)]$	0.99973	0.99922	0.99359
$\sigma[\mathrm{Re}(\lambda)]$	0.01320	0.01199	0.01166
$\sigma[\mathrm{Im}(\lambda)]$	0.01099	0.01047	0.01614
$E[\mathrm{Re}(A)]$	-0.04565	-0.01162	-0.04928
$E[\mathrm{Im}(A)]$	-0.98511	-1.10340	-1.03602
$\sigma[\mathrm{Re}(A)]$	0.224	0.180	0.180
$\sigma[\mathrm{Im}(A)]$	0.214	0.165	0.142

Table 8: Statistical results of the identification, structural damping, g=0.10, U=1,l=-0.050+0.99875i, A=-1.00125i, e=0.2, Dw=zW.

4 CONCLUSIONS

The linear least squares procedure developed here addresses the task of identifying the modal eigenvalue and residue corresponding to a state-space modal description of a system with arbitrary viscous damping. The procedure is an SDOF technique that assumes that the FRF contribution of modes other than the one in focus are negligible. In the case of a one-degree-of-freedom system without noise the results are exact. For data that is contaminated with noise, overdetermined equations are obtained when complex FRF values for more than two excitation frequencies are used in the least squares procedure. In order to obtain the best results with noisy data, the FRF values were selected from points in the vicinity of the peak FRF magnitude.

A series of statistical evaluations of analytical data considered data contaminated with a specific noise level, scaled relative to the peak FRF. The trials considered the effect of using various sampling intervals and cutoffs that define the frequency interval from which the FRF values are selected. It was found that the best results were obtained if the frequency sampling increment is selected to be one quarter of the modal bandwidth, and the data values are selected from the interval over which the FRF magnitude exceeds -6 dB relative to the peak, which corresponds to the quarter-power points. Using FRF val-

$\delta(dB)$	-3	-6	-9
N (average)	4.03	7.70	16.13
$E\left[\mathrm{Re}\left(\lambda\right)\right]$	-0.04955	-0.04936	-0.04788
$E\left[\mathrm{Im}\left(\lambda\right)\right]$	1.00333	0.99964	1.00166
$\sigma\left[\mathrm{Re}\left(\lambda\right)\right]$	0.01058	0.00795	0.00790
$\sigma\left[\mathrm{Im}\left(\lambda\right)\right]$	0.01088	0.00745	0.00847
$E\left[\mathrm{Re}\left(A\right)\right]$	-0.08375	-0.03674	-0.09416
$E\left[\mathrm{Im}\left(A\right)\right]$	-1.02469	-1.04355	-1.05872
$\sigma\left[\mathrm{Re}\left(A\right)\right]$	0.214	0.113	0.102
$\sigma\left[\mathrm{Im}\left(A\right)\right]$	0.201	0.103	0.081

Table 9: Statistical results of the identification, structural damping, g=0.10, U=1,l=-0.050+0.99875i, A=-1.00125i, e=0.2, Dw=0.5zW.

ues that fall below this cutoff was shown to decrease the quality of the estimates, apparently because the signal to noise ratio for such points is lower. A finer sampling interval was not considered, but it is reasonable to conjecture that the results would improve in that case.

The evaluations demonstrated that the smallest error is obtained for the imaginary part of the eigenvalue, which is essentially the undamped natural frequency if damping is light. The error for the estimated imaginary part of the eigenvalue, which is proportional to critical damping ratio, was greater than the real part, and the error for both parts of the residue were largest. However, these errors as a fraction of the correct value, were always lower than the noise ratio. Furthermore, at the optimal sampling rate and frequency cutoff, the ratio of the standard deviation of each quantity to the mean value was substantially lower than the noise ratio.

The linear least squares scheme was shown to be equally effective at identifying the modal damping ratio corresponding to a structural damping model. The primary reason the technique was developed was to expedite the AMI identification procedure [7], [8] which performs an MDOF identification by iterating on SDOF fits to the FRF data. Used on its own for FRF data of a multi-degree-of-freedom system, the present technique is limited by the assumption that each mode is dominant in the vicinity of its resonance, which is an attribute it shares with other SDOF schemes. This is often the case for the low frequency modes, especially if the structure is not too complex. A comparison of results obtained by the present procedure to those obtained from a commercial modal analyzer are provided in a companion paper [6]. However, even for systems where some modes are close, linear least squares SDOF offers a quick qualitative check of MDOF identification results in selected frequency ranges.

References

[1] **Ewins, D. J**., *Modal Testing: Theory, Practice and Applications,* Second Edition, Research Studies Press Ltd., Baldock, Hertfordshire, England, 2001.

[2] **Maia, S., Silva, J. M. M., He, J., Lieven, N. A. J., Lin, R. M., Skingle, G. W., To, W. M., Urgueira, A. P. V.**, *Theoretical and Experimental Modal Analysis,* Research Studies Press Ltd., Taunto, Somerset, England, 226-227.

[3] **Phillips, A. W., Allemang, R. J.**, *Single Degree-of-Freedom Modal Parameter Estimation Methods*, Proceedings of the 14th International Modal Analysis Conference, Dearborn, MI, 253-260, 1996.

[4] **Drexel, M. V., Ginsberg, J. H.,** *Exact evaluation of natural frequency and damping ratio from a frequency response curve*, ASME J. of Vibration and Acoustics, 123, 403-405, 2001.

[5] Fill in ????

[6] **Allen, M., Moloney, C., Ginsberg, J. H., Ferri, A.**, *Comparison of a Linear Least Squares Method and STAR Modal's SDOF Results for a Square Elastic Plate*, Proceedings of the 21st International Modal Analysis Conference, Orlando, FL, 2003.

[7] **Ginsberg, J. H., Zaki, B. R., Drexel, M. V.**, *Application of the Mode Isolation Algorithm to the Identification of a Complex Structure,* Proceedings of the 20th International Modal Analysis Conference, Los Angeles, CA, 2002.

[8] **Drexel, M. V., Ginsberg, J. H., Zaki, B. R.,** *State Space Implementation of the Algorithm of Mode Isolation,* ASME Journal of Vibrations and Acoustics, forthcoming**,** 2002.